Supplementary Materials

1 The RAQMS model

Chemical and aerosol forecasts from the Real-Time Air Quality modeling System (RAQMS) where used for flight planning activities during ARCPAC. RAQMS is a unified (stratosphere/troposphere), online (meteorological, chemical, and aerosol) modeling system which has been developed for assimilating satellite observations of atmospheric chemical composition and providing real-time predictions of trace gas and aerosol distributions (Pierce et al., 2007, 2009). The chemical formulation follows a family approach with partitioning on the basis of photochemical equilibrium approximations. The non-methane hydrocarbon (NMHC) chemical scheme is based on the carbon bond lumped structure approach (Pierce et al., 2007). The RAQMS aerosol model incorporates online aerosol modules from GOCART (Chin et al., 2003). Seven aerosol species ($SO_4^=$, hydrophobic and hydrophilic organic carbon (OC), and black carbon (BC), dust, sea-salt) are transported. RAQMS biomass burning emissions use twice daily ecosystem/severity based emission estimates coupled with MODIS Rapid Response fire detections (Al-Saadi et al., 2008).

The RAQMS chemical and aerosol analysis during ARCPAC were conducted at 2˚×2˚ horizontal resolution and included real-time assimilation of cloud-cleared Ozone Monitoring Experiment (OMI) total column O_3 measurements, and stratospheric O_3 profiles from the Microwave Limb Sounder (MLS) on the NASA Aura satellite. MODIS aerosol optical depth (AOD) retrievals from instruments onboard the Terra and Aqua satellites were also assimilated. A Mie code based look-up table of speciated aerosol mass extinction coefficients and relative humidity dependent hydroscopic growth factors was used to convert the predicted aerosol mass to speciated extinction, which is integrated vertically to obtain a first guess AOD for assimilation. During the chemical and aerosol assimilation cycle the RAQMS meteorological forecasts are reinitialized from NOAA Global Forecasting System (GFS) analyses at 6 h intervals.

2 Movies of RAQMS constituent evolution and transport

Three Quicktime® movies are available in compressed format. The first movie (RAQMS_April_2008_290K_BCOC.mov) shows particulate BC/OC from all sources, the second (RAQMS_April_2008_290K_SO4.mov) particulate $SO_4^=$ from all sources, and the third (RAQMS_April_2008_290K_Dust.mov) dust. In each case, the color scale shows the concentration of the consituent of interest on the 290K potential temperature surface. White contour lines show the pressure (hPa) of the 290K isentrope, which intersects the surface (bold white) over southeastern and central Asia and is in the middle tropopshere (where most haze layers were observed) over the Arctic. The ARCPAC NOAA WP-3D flights are shown in bold white.

3 Movies of FLEXPART BB and fossil fuel CO

Three Quicktime® movies showing FLEXPART simulations of CO transport are available. In the first movie (NH_BB_column_CO_mg_m2_IR.mov), contours indicate the column mass (mg m^{-2}) of a FLEXPART passive CO tracer emitted from biomass burning sources (cyan squares) as indicated by MODIS Hotspot Active Fire Detections (made available by the Food and Agriculture Organization of the United Nations (UN-FAO), in partnership with the University of Maryland and NASA MODIS Rapid Response). The underlying infra-red satellite images depict the temperature of the Earth's surface and clouds with blues and greens indicating warmer temperatures and yellows and reds indicating cooler temperatures. These Arctic composite images are produced from geostationary and polar orbiting satellite retrievals by the Space Science and Engineering Center, University of Wisconsin-Madison (funded by the Arctic Natural Science Program, Office of Polar Programs, National Science Foundation Grant ARC-0713843).

In the second movie (NH_anthro_column_CO_mg_m2_IR.mov), contours indicate the column mass (mg m^{-2}) of a FLEXPART passive CO tracer emitted from anthropogenic sources in Europe, Asia and North America according to the EDGAR 3.2 Fast Track 2000 data set, which estimates year 2000 emissions using the EDGAR 3.2 estimates for 1995 and trend analyses for the individual countries. EDGAR uncertainty estimates are roughly 50% or greater [Olivier and Berdowski, 2001].

The third FLEXPART movie (FLEXPART_BB_CO.mov) shows images of BB emissions and transport as depicted in Fig. 10. Colors are column-integrated values of a 20-day conserved CO tracer emitted by BB sources.

4 Methods and uncertainties for aerosol size distributions during ARCPAC

Size distributions were measured using 3 instruments during ARCPAC. Particles with diameters from ~0.004 to 0.07 μm were measured with a 5-channel condensation particle counter (CPC), the nucleation-mode aerosol size spectrometer NMASS (Brock et al., 2000). Particles with diameters from 0.07 to ~0.8 μm were measured by an ultra-high sensitivity aerosol spectrometer UHSAS (Cai et al., 2008) operating behind a 1 μm aerodynamic diameter impactor with an substrate coated wih Apiezon Type L grease. Particles with diameters from ~0.7 to 8.9 μm were measured with a custom-built white-light optical particle counter (WLOPC). The UHSAS and WLOPC sampled in the cabin downstream of the low-turbulence inlet (LTI, Wilson et al. 2004), while the NMASS sampled from a double diffusing inlet in a non-pressurized wing pod. The UHSAS was operated in serial downstream of the dry channel (<10% relative humidity) of the cavity ringdown aerosol extinction spectrometer. The WLOPC sample stream was maintained at a relative humidity <40% by heating the sample line.

4.1 UHSAS high gain failure

On two flights during ARCPAC, 2008/04/15 and 2008/04/18, the high gain amplifier of the UHSAS failed for a portion of the flight. These data are irretrievably lost. The times of the failures are from 11:38:52 UTC onward on 2008/04/15, and prior to 01:03:27 on the flight of 2008/04/18.

4.2 UHSAS mass flow controller sensitivity to altitude

The sample flow into the UHSAS instrument is controlled and measured by a mass flow controller that is mounted on the exhaust side of the sample pump. This exhaust mass flow controller was calibrated on the ground before ARCPAC, and the nominal flow rate checked on the ground during the project. After ARCPAC, it was noted that agreement

between the NMASS instrument, which measures all particles larger than ~0.004 μm, was not within expected uncertainties of UHSAS concentrations in cases where all particles were large and should have been measured equally well by both instruments. The mass flow controller (MFC) was then calibrated as a function of sample pressure. The MFC was found to have a pressure dependency that resulted in flow variations of ~30% over the altitude range of the aircraft. There was a consistent discrepancy in concentration between the NMASS and UHSAS as a function of pressure throughout the mission.

To try to correct for this large artifact, we have chosen all times in flight in the Arctic when all particles were present in the accumulation mode and should have been counted with unit efficiency by both the NMASS and UHSAS. We have corrected the UHSAS concentrations based on a regression between static pressure and the ratio between the NMASS and UHSAS concentrations (Fig. S1). We estimate the uncertainty in the UHSAS MFC flow as being the sum in quadrature of the basic flow calibration uncertainty for the NMASS and UHSAS, the uncertainty in the regression of the correction curve to the UHSAS flow, and the root-mean-squared deviation of the datapoints from the fit in Fig. S1. The manufacturer's stated accuracy for the MFC is 0.8% + 0.2%×FS, where FS is 3.333 cm^3 s^{-1}. Typical readings of flow were 0.8 cm^3 s^{-1}, so expected accuracy is 1.6%. The total uncertainty in the NMASS concentration is estimated to be 8% based on repeated calibrations between the NMASS and a laboratory CPC which is calibrated using charged particles and an electrometer. The uncertainty in the pressure correction term for the UHSAS is estimated as two times the root-mean-squared residual deviation of the data from the fitted curve in Fig. S1; this uncertainty is 14.6%. There are no substantial biases in this deviation. The above errors propagated in quadrature sum to 16.7%. This is a concentration uncertainty, and does not include potential sizing uncertainties, which are described below. To this concentration uncertainty will be added an additional uncertainty due to flow transients during altitude changes as discussed below.

4.3 Transient UHSAS sample flow response to pressure changes

The UHSAS, a commercial instrument, has a total internal instrument volume (optics block, pump, plumbing, filters) estimated to be approximately 1 liter. The aerosol sample flow enters this volume through a small focusing nozzle. The aerosol sample flow rate is not directly measured; instead, the exhaust of the instrument is controlled by a mass flow controller. As the aircraft ascends or descends the mass of air within the instrument must decrease or increase, respectively. The only source for this mass change is through the aerosol inlet, since the exhaust flow controller holds a constant mass flow rate. For example, higher-than-expected inlet mass flows must occur throughout descent, even while the exhaust mass flow controller indicates a constant flow rate. The particle concentration appears to be higher during descents, since more air (and more particles) are entering than expected based on readings from the exit mass flow controller. The opposite is true during ascents. A correction to this issue would be easily calculable, except that the inlet nozzle restricts the airflow entering the optics block, so that there is a time lag between any pressure change and the equilibrium pressure within the UHSAS instrument; this lag is dependent upon the rate of pressure change and the fluid dynamics of the nozzle flow, which is Reynolds number dependent. The transient sample flow effect can be remedied only by directly measuring the sample flowrate entering the instrument, which we intend to do in future projects. We expect that other UHSAS benchtop units (those not within cloud probe canisters) flown on research aircraft exhibit similar sample flowrate problems.

To approximately correct for these flow transients, we have applied a correction of +15% and -8% to UHSAS concentrations during aircraft ascents and descents, respectively, based upon observed discrepancies in aerosol concentrations measured by the UHSAS and NMASS (Fig. S2). The residual artifact in the concentration remaining after the ascent/descent flow correction is estimated as up to +10/-5% during ascents, and +5/-10% during descents.

4.4 UHSAS counting statistics

We estimate the uncertainty caused by particle counting statistics during the one-second sample time based upon representative particle size distributions for the different environments encountered during ARCPAC. For a very few cases encountered, particle concentrations were <30 cm^{-3}, the uncertainties were as large as 22%. Much more typical (>91% of data on the least polluted Arctic flight, 2008/04/12) concentrations were >200 cm^{-3}, in which case counting statistics produced uncertainties <8%.

4.5 UHSAS sizing uncertainties

The particle surface area and volume calculated from the UHSAS measurements depend not only upon the counting accuracy of the instrument, but also upon the sizing accuracy. The instrument is calibrated using ammonium sulfate particles, since their refractive index at 1.053 μm lies in the middle of the typical range of refractive indices for atmospheric fine particles composed of mixed sulfate salts and organic components. As composition (and hence refractive index) of the atmospheric aerosol changes, the sizing accuracy of the UHSAS will also change. We estimate the uncertainty in the surface area and volume based upon a simulation of the scattering within the instrument using Mie theory. Current understanding of the refractive index of organic material from secondary organic aerosol formation and from biomass burning sources particles suggests a likely range in the real component of the refractive index of ~1.41-1.56 with imaginary components of <0.01i at infrared wavelengths. Accounting for inorganic matter on the particles, we use a real refractive index range of 1.43-1.56 for estimating the sizing uncertainties due to refractive index variation (Fig. S3). For particle diameters <0.5 μm, which encompass most of the mass and surface area, the actual diameter may deviate from the measured diameter by +8/-4%. Since this is a potential bias rather than a random uncertainty, the errors propagate directly to surface as +17%/-8%, and to volume as +26/-12%. We have not considered the possible role of incandescence and evaporation of BC particles in the UHSAS, although evidence for this has been observed in the laboratory for nearly pure BC particles (B. Weinzierl, personal communication, 2009).

4.6 Error propagation from inversion of NMASS data

The NMASS measures the concentration of all particles larger than a given diameter using five discrete CPCs that have 50% counting efficiencies of 0.005, 0.008, 0.015, 0.030, and 0.055 μm. These data are combined with the UHSAS data using nonlinear inversion technique to recover a size distribution from 0.004-0.07 μm (Brock et al., 1999). The ability of this method to accurately retrieve size distributions is evaluated by a Monte Carlo simulation of the inversion solution while perturbing the input data with experimental uncertainties. For ARCPAC, seven representative size distributions that span the range of observations were tested in the Monte Carlo simulation. Each test case was simulated 1000 times, and the deviation of the retrieved number, surface and volume from the known input size distribution was evaluated. The mean deviation for particle number was a positive bias of +2.8% with a standard deviation of 8.6%; for surface area these values were +0.7% and 1.1%, and for volume they were +0.3% and 0.3% (very little volume is present in the NMASS size range). The uncertainty in total particle number that is caused by inversion uncertainty in the concentration of particles with diameters <0.07 μm is +5.8%/-11.4%. Inversion-caused uncertainties are considered negligible for surface and volume compared with UHSAS uncertainties.

4.7 Total uncertainties in fine particle number, surface, and volume

Fine particle number concentration uncertainties stem from the concentration uncertainty from the UHSAS following pressure-dependent flow correction, counting statistics, and uncertainties in the concentration due to the inversion. For typical ARCPAC arctic conditions, these sum in quadrature to yield +19%/-22%. During ascents there is an additional potential bias of +10/-5% added, and during descents +5/-10% is added. Uncertainties in surface area and volume include the concentration uncertainties combined linearly with uncertainties from sizing biases, yielding +36%/-27% for surface area and +45%/-31%. During ascents there is an additional potential bias of +10/-5% and during descents +5/-10%.

4.8 Uncertainties in coarse particle measurements

Uncertainties in the WLOPC are caused primarily by counting statistics and by sizing uncertainties. Typical coarse particle concentrations were <1 cm^{-3}, leading to statistical uncertainties in total coarse number concentration >12% at the flow rate of ~60 cm^{-3} s^{-1}. The uncertainty in number is much worse as particle size increases and particle number concentration falls, leading to very large statistical fluctuations in particle surface and volume. For example, most of the volume is in particles with diameters >1.5 μm, and the typical concentrations of particles in this size range were <0.1 cm^{-3}, leading to +/-40% statistical fluctuations in 1-second number concentrations. Coarse particle counting uncertainties are reduced to <10% by averaging to 30 s, as was done in the archived data and in the data used in this manuscript. A very few larger particles can contribute substantially to particle surface and volume, however, indicating that yet longer averaging times might be needed to reduce statistical fluctuations in these parameters. Flow calibration uncertainty is ~5%.

Sizing uncertainties for the WLOPC lead to additional uncertainties in particle surface are and volume. These are difficult to quantify, since the particle refractive index is unknown, and since the shape may not be spherical. Calibration repeatability is ~5% in diameter, and variations in particle size due to refractive index changes, based on Mie simulations of the instrument response, are estimated to be +15% /-7% at the peak of the volume distribution (~3 μm), leading to surface and volume uncertainties of +32/-14% and +52/-20%, respectively. Resulting total estimated uncertainties in 30-s coarse particle number concentrations are +/- 11%, in coarse surface areas +48/-30%, and in coarse volumes +73/-41%.

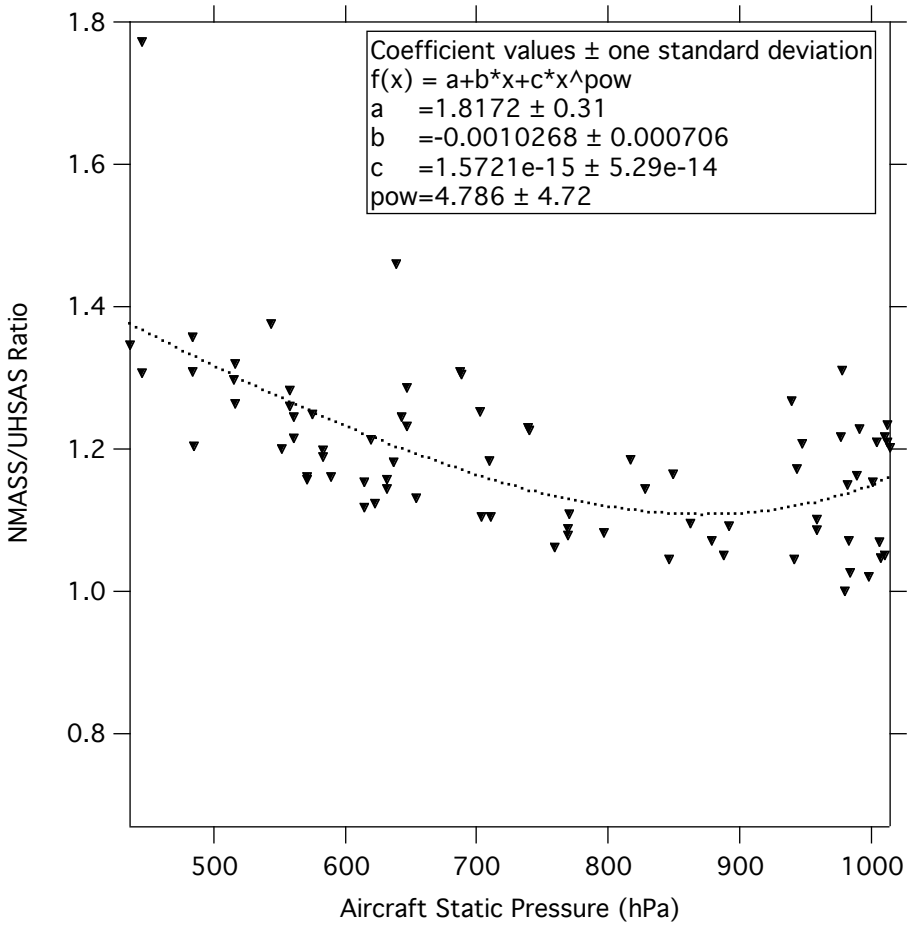

Figure S1. Ratio of concentration of particles with diameters >0.05 μm from the NMASS to the total UHSAS concentration for periods of level flight when all particles are believed to be in the UHSAS size range, as a function of ambient static pressure. The curve is the parameterization used to correct the flow rate of the UHSAS.

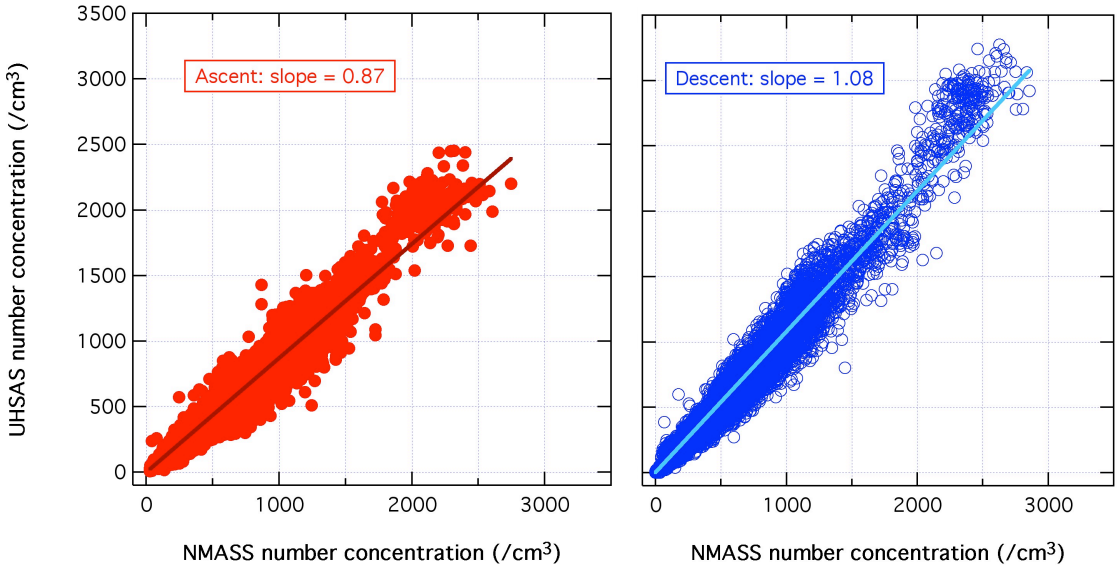

225

226 Figure S2. UHSAS concentration plotted as a function of NMASS concentrations during
227 ascents and descents prior to correction. The slope is the correction applied to the data.

228

228

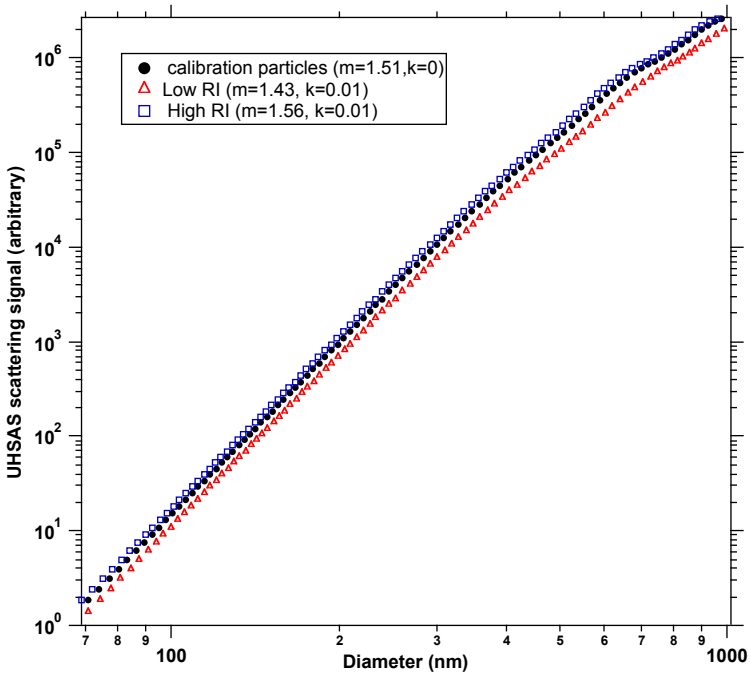

229

230 Figure S3. Calculated scattered light intensity integrated over the UHSAS optical
231 geometry as a function of particle diameter for three different refractive indices that span
232 the range of likely values in the Arctic environment during ARCPAC. Each point is a
233 sizing bin in the UHSAS.

234 Table S1. Scientific objectives and methods of ARCPAC.

Goals	Specific questions	Approaches
Improve understanding of the chemical, optical, and microphysical characteristics of aerosols in the Arctic in springtime.	• What is the visible extinction and absorption of the aerosol, and how do these properties vary with relative humidity? • What is the mass concentration and size distribution of BC? • To what extent are BC particles coated with other materials, and do such coatings influence the radiative and cloud-nucleating properties of the BC particles? • What is the contribution of organic material to the optical and chemical properties to the aerosol? • How do aerosol concentrations, composition, optical properties, and cloud nucleating properties above the surface relate to values measured at the surface? • What are the radiative forcings and resulting atmospheric heating rates due to the aerosol, and how do these values compare with those derived from airborne lidar, surface lidar, and surface aerosol measurements? • How do the composition and hygroscopic properties of aerosols relate to chemical processing estimated from trace gases?	• Use airborne and remote-sensing measurements since properties aloft are likely decoupled from ground measurements. • Make fast-response remote sensing and in situ measurements because of extreme vertical stratification and non-uniform distribution. • Make accurate and precise measurements of aerosol extinction, absorption, size distribution, composition, BC number and mass, and irradiance. • Measure the variation in optical properties with relative humidity to accurately determine radiative forcing. • Using multi-platform irradiance measurements, determine flux divergence and heating rates; compare with radiative transfer models constrained by in situ measurements
Determine the source types (industrial, urban, biomass, dust, sea-salt) of the aerosol components, especially absorbing components.	• What are the correlations between aerosol components and trace gases? • How does the composition of the aerosol and trace gases compare to that expected from transport and emission models such as FLEXPART and chemical transport models such as RAQMS? • Does the vertical distribution of aerosol properties reflect differences in source region, transport, and removal? • What are the major sources that contribute to atmospheric and surface BC during the critical springtime warming period?	• Make fast-response measurements of key gas-phase and aerosol species to help identify sources. • Use transport and coupled transport/chemistry models to relate the observed aerosol and gas-phase characteristics to sources and transport mechanisms and to evaluate their importance. • Where possible, couple measurements to long-term, ground-based sites to link to established climatologies
Determine the microphysical and optical characteristics of representative stratiform clouds in the lower Arctic troposphere in springtime, and evaluate if pollution particles affect these cloud properties.	• What is the number density of CCN present in aerosol layers and in clean air, and is there closure between measured CCN and that predicted from the observed aerosol composition and size distribution? • How does the number concentration of CCN, as a function of water supersaturation, vary as a function of altitude? • Is the cloud droplet number concentration in liquid and mixed-phase clouds consistent with that predicted from the observed CCN and cloud cooling rate? • What are the measured solar reflectance and transmission, the IR irradiance, and the effective radius of Arctic clouds, and how do these values vary with CCN and concentration and cloud particle phase?	• Measure CCN, aerosol size distribution and composition, and cloud radiative properties above and below stratiform clouds • Use non-soluble gas-phase tracers to correlate aerosol properties outside cloud to determine in-cloud initial values • Use LES and parcel models to elucidate the mechanisms of aerosol perturbation to cloud microphysical and optical properties • Compare observed and modeled values of cloud microphysical and radiative properties

	• How do directly measured and derived cloud properties compare with remotely measured and derived parameters at the DOE ARM site?	
Improve understanding of halogen chemistry and O_3 budget in the lower troposphere of the Arctic	• What is the distribution of gas phase chlorine and bromine compounds? • What is the vertical distribution of sea-salt aerosol and what chemical processing has it undergone? • What is the relative importance of the sources of O_3 in the Arctic and subArctic lower troposphere in springtime (production vs. stratospheric vs. long-range transport)?	• Use new in situ techniques to measure Br_2, BrCl, Cl_2, and BrO • Sample at low altitude (<100 m) over differing snow and ice surfaces, open leads, ice-filmed leads, and land • Use tracer correlations to evaluate O_3 sources and sinks

235

236